The Journal of Neuroscience, March 1, 1999, *19*(5):1566–1576

Developmental Synaptic Changes Increase the Range of Integrative Capabilities of an Identified Excitatory Neocortical Connection

María Cecilia Angulo,[1] Jochen F. Staiger,[2] Jean Rossier,[1] and Etienne Audinat[1]

[1]*Neurobiologie et Diversité Cellulaire, Centre National de la Recherche Scientifique, Unité Mixte de Recherche 7637, Ecole Supérieure de Physique et de Chimie Industrielles de la ville de Paris, 75231 Paris Cedex 5, France, and* [2]*Heinrich-Heine University, C & O Vogt Institute for Brain Research, D-40001 Düsseldorf, Germany*

Excitatory synaptic transmission between pyramidal cells and fast-spiking (FS) interneurons of layer V of the motor cortex was investigated in acute slices by using paired recordings at 30°C combined with morphological analysis. The presynaptic and postsynaptic properties at these identified central synapses were compared between 3- and 5-week-old rats. At these two postnatal developmental stages, unitary EPSCs were mediated by the activation of AMPA receptors with fast kinetics at a holding potential of −72 mV. The amplitude distribution analysis of the EPSCs indicates that, at both stages, pyramidal–FS connections consisted of multiple functional release sites. The apparent quantal size obtained by decreasing the external calcium ($[Ca^{2+}]_e$) varied from 11 to 29 pA near resting membrane potential. In young rats, pairs of presynaptic action potentials elicited unitary synaptic responses that displayed paired-pulse depression at all tested frequencies. In older animals, inputs from different pyramidal cells onto the same FS interneuron had different paired-pulse response characteristics and, at most of these connections, a switch from depression to facilitation occurred when decreasing the rate of presynaptic stimulation. The balance between facilitation and depression endows pyramidal–FS connections from 5-week-old animals with wide integrative capabilities and confers unique functional properties to each synapse.

Key words: paired recordings; pyramidal cell; interneuron; synaptic plasticity; depression; facilitation; basket cell; fast-spiking cell; glutamate release

Activity-dependent mechanisms dynamically regulate the efficacy of synaptic transmission and the strength of a given synapse largely results from the activity it has previously experienced. Short-term changes that adjust the synaptic gain according to recent activity have been described at most synapses. After a single action potential or a train of action potentials in the presynaptic axon, the subsequent postsynaptic responses that occur during the following hundreds of milliseconds can be either facilitated or depressed. These activity-dependent modulations of synaptic responses depend largely on presynaptic mechanisms (Zucker, 1989; Stevens and Wang, 1995), the development of which, however, is also influenced by the identity of the postsynaptic targets. In invertebrates (Muller and Nicholls, 1974; Davis and Murphey, 1993; Katz et al., 1993) and in the mammalian peripheral (Koerber and Mendell, 1991) and CNSs (Thomson, 1997; Markram et al., 1998; Reyes et al., 1998; Scanziani et al., 1998), different terminals from the same presynaptic axon may constitute either facilitating or depressing synapses according to the target cells. The facilitating or depressing characteristics of a synapse will greatly influence how the firing rates and the temporal pattern of presynaptic action potentials are transferred to postsynaptic neurons (Tsodyks and Markram, 1997).

Within the neocortex, information processing relies on the synaptic interactions involving pyramidal and nonpyramidal cells. Pyramidal cells are excitatory glutamatergic neurons that convey the output signals of the neocortex but also provide most of the intracortical excitatory synaptic drive. Nonpyramidal cells are mainly inhibitory local circuit neurons using GABA as neurotransmitter. Excitatory responses at synapses between neocortical pyramidal cells are characterized by a frequency-dependent depression during discharges of pairs or trains of presynaptic action potentials, whereas synapses from pyramidal cells onto interneurons can display either facilitation or depression (Thomson et al., 1993; Deuchars et al., 1994; Buhl et al., 1997; Markram et al., 1997; Thomson, 1997; Galarreta and Hestrin, 1998; Reyes et al., 1998). This heterogeneity among pyramidal–interneuron synapses is probably caused by the diversity of nonpyramidal cells, which has made difficult the characterization of synaptic and integrative properties of specific subtypes of interneurons (Kawaguchi, 1993, 1995; Cauli et al., 1997; Parra et al., 1998).

We focused our attention on the excitatory synapses made by pyramidal cells onto a discrete subtype of neocortical interneuron. These interneurons, called fast-spiking (FS) cells, can be identified by their ability to fire fast action potentials at high nonaccommodating frequencies (McCormick et al., 1985; Kawaguchi, 1993; Cauli et al., 1997). Most of these cells express the calcium-binding protein parvalbumin (Kawaguchi, 1995; Cauli et al., 1997), and their axons form multiple axoaxonic (chandelier cells) or axosomatic (basket cells) contacts (Kawagu-

Received Oct. 8, 1998; revised Dec. 7, 1998; accepted Dec. 9, 1998.

This study was supported by Centre National de Recherche Scientifique (France), European Union Grants 96–0589 and 96–0382, and Deutsche Forschungsgemeinschaft Grant STA 431/2–1. M.C.A. was supported by a fellowship from Instituto Colombiano de Ciencia y Tecnología (Colciencias; Colombia). We thank Samia Ben Ammou and U. Opfermann-Emmerich for technical assistance and Drs. Serge Charpak and James T. Porter for helpful comments on this manuscript.

Correspondence should be addressed to Dr. Etienne Audinat, Neurobiologie et Diversité Cellulaire, Centre National de la Recherche Scientifique, Unité Mixte de Recherche 7637, Ecole Supérieure de Physique et de Chimie Industrielles, Paris, 10 rue Vauquelin, 75231 Paris Cedex 5, France.

Table 1. Action potential firing and unitary EPSC properties of postsynaptic FS interneurons at two different developmental stages

	Connections from 3-week-old rats mean ± SD (*n*)	Connections from 5-week-old rats mean ± SD (*n*)
Postnatal days	17 ± 1 (36)	33 ± 2 (21)
Firing Properties[a]		
Early accommodation	15 ± 15% (36)	12 ± 13% (20)
Late accommodation	3 ± 10% (36)	4 ± 9% (20)
Spike amplitude (A)	78 ± 8 mV (36)	81 ± 5 mV (20)
Spike duration ($t_{1/2}$)	0.4 ± 0.1 msec (36)	0.31 ± 0.06 msec (20)
AHP	−21 ± 3 mV (36)	−25 ± 3.3 mV (20)
R_{in}	0.16 ± 0.06 GΩ (36)	0.14 ± 0.04 GΩ (20)
V_{rmp}	−73 ± 8 mV (34)	−76 ± 3.1 mV (20)
Unitary EPSCs		
Latency	0.47 ± 0.28 msec (36)	0.54 ± 0.26 msec (21)
1st exponential decay (τ_1)	1.3 ± 0.5 msec (22)	1.3 ± 0.6 msec (15)
Amplitude of τ_1	88 ± 12% (22)	89 ± 7% (15)
2nd exponential decay (τ_2)	11 ± 6 msec (22)	17 ± 15 msec (15)
Amplitude of τ_2	12 ± 12% (22)	11 ± 7% (15)
τ[b]	1.7 ± 0.5 msec (13)	1.7 ± 0.4 msec (4)
NBQX/DNQX Block (−72 mV)	98 ± 2% (5)	96.5% and 99.2% (2)

[a] There were no statistical differences of action potential and firing kinetics between 3- and 5-week-old rats, except for $t_{1/2}$ and AHP ($p < 0.05$; Student's *t* test).
[b] mean τ of EPSCs well fitted with a single exponential function.

chi, 1995) preferentially on pyramidal cells. This morphological feature suggests a powerful role of FS cells in regulating the neocortical output. The control of FS cell activity and, therefore, their integration of excitatory inputs is likely to play a major role in balancing excitation and inhibition and/or in maintaining temporal coherence in the cortical network (Cobb et al., 1995; Whittington et al., 1995; Buzsaki, 1997).

In the present work, we first characterized the basic presynaptic and postsynaptic properties at the pyramidal cell to FS interneuron connection in layer V of the rat motor cortex. We then studied the paired-pulse response characteristics at this central synapse. Our results show that in 3-week-old rats, pyramidal–FS identified synapses depress at all tested frequencies. In contrast, paired-pulse depression (PPD) and paired-pulse facilitation (PPF) coexisted in connections from 5-week-old rats, indicating that the range of integrative capabilities largely increased after the third postnatal week.

MATERIALS AND METHODS

Brain slice preparation. Wistar rats [postnatal days 14–20 (P14–P20) and P27–P36] were anesthetized by an intraperitoneal injection of ketamine (65 mg/kg) and xylazin (14 mg/kg) and decapitated. Brains were quickly removed, and 300-μm-thick parasagittal sections of cerebral motor cortex were prepared as previously described (Cauli et al., 1997). The slices were incubated for 1 hr in a physiological extracellular saline solution containing (in mM): NaCl, 121.0; KCl, 2.5; NaH_2PO_4, 1.25; $CaCl_2$, 2; $MgCl_2$, 1; $NaHCO_3$, 26; glucose, 20; and pyruvate 5, and bubbled with a mixture of 95% O_2 and 5% CO_2. For recordings, they were transferred to a chamber and perfused at 1–2 ml/min with the same physiological extracellular saline solution at 30°C.

Paired recordings. Paired recordings from synaptically coupled pyramidal and FS neurons were obtained by using sharp intracellular and patch microelectrodes, respectively.

Postsynaptic FS cells were initially identified using videomicroscopy with Nomarski optics under infrared illumination (Stuart et al., 1993). Neurons with pyramidal or bipolar-like shapes were excluded from the sample. Furthermore, the kinetics of the action potential firing of recorded cells was analyzed to take into account only those with electrophysiological patterns of FS cells (see data collection and analysis; Connors and Gutnick, 1990; Kawaguchi, 1995; Cauli et al., 1997). Patch pipettes were pulled from borosilicate glass tubing and had a resistance of 3–5 MΩ when filled with an internal solution containing (in mM): 144 K-gluconate, 3 $MgCl_2$, 0.2 EGTA, and 10 HEPES, pH 7.2–7.4, 300 mOsm. Two milligrams per milliliter biocytin was also included to study the morphology of postsynaptic cells (see Morphology). In 20 experiments, we used 100 μM spermine and, in five experiments, we used 4 mM ATP and 0.4 mM GTP into the patch pipette. We did not observe any difference between recordings performed with and without these compounds for the parameters measured in the present work.

Whole-cell recordings were performed from layer V FS interneurons. The holding potential was set to −60 mV on the patch-clamp amplifier for all postsynaptic interneurons that gave a membrane potential of −72 mV after correction for junction potentials (Neher, 1992). Only cells with resting membrane potentials more negative than −50 mV were further considered.

Unitary EPSCs were studied in control conditions and after adding AMPA/kainate antagonists DNQX or NBQX in the external solution (10 μM; Tocris Cookson, Bristol, UK). In experiments in which the $[Ca^{2+}]_e$ was reduced from 2 or 3 mM to 0.5 mM, the external $[Mg^{2+}]_e$ was increased to 2.5 mM.

After whole-cell recordings were established, presynaptic neurons were impaled with a sharp microelectrode filled with 3 M KCl or 1.5 M KCl and 2% biocytin (resistance, 40–120 MΩ). Pyramidal cells were initially identified by their characteristic action potential firing induced by depolarizing current pulses (McCormick et al., 1985; Connors and Gutnick, 1990; Cauli et al., 1997). The identification of the presynaptic cells was further confirmed by their characteristic features obtained by biocytin labeling (see Morphology). The impaled presynaptic cells were iontophoretically injected with biocytin by applying depolarizing current pulses at the end of the experiment (2–3 nA, 5–15 min). Postsynaptic responses were induced by triggering action potentials in the presynaptic cell with depolarizing pulses (3 msec, 1.5 nA). The latency of these responses was measured from the peak of the presynaptic action potential. Monosynaptic coupling between the two neurons were considered when EPSCs were elicited with brief latencies (Table 1). The stability of the recordings during the time course of the experiment was tested by plotting the EPSC amplitudes against time. A run down of the synaptic responses was rarely observed. In our experimental conditions, the peak amplitude and the probability of response of the EPSCs could remain stable for up to 3 hr of recording.

Data collection and analysis. Whole-cell current-clamp (mode I-Clamp fast) and voltage-clamp recordings of postsynaptic FS cells were obtained using a patch-clamp amplifier (Axopatch 200A; Axon Instruments, Foster City, CA) and filtered at 5 and 2 kHz, respectively. Series resistances between 10 and 25 MΩ were monitored throughout the experiments, but they were not compensated. Intracellular current-clamp recordings of

presynaptic pyramidal cells were obtained using an intracellular amplifier (Neuro Data; Instruments Corp.). Digitized data were acquired and analyzed off-line using Acquis1 software (Gérard Sadoc, Centre National de la Recherche Scientifique, Gif-sur-Yvette, France).

The characteristics of the action potential discharges of postsynaptic cells were analyzed after the procedure described by Cauli et al. (1997). The accommodation parameters were measured on discharges elicited by application of 800 msec depolarizing current pulses. The instantaneous discharge frequency was determined throughout the discharge and plotted as a function of time at the different stimulation intensities. The instantaneous discharge frequencies between the first two spikes ($f_{initial}$), 200 msec after the beginning of the discharge (f_{200}), and at the end of the stimulation (f_{final}) were then measured at the highest intensity tested (550–1200 pA). Early and late accommodations were calculated according to $(f_{initial} - f_{200})/f_{initial}$ and $(f_{200} - f_{final})/f_{initial}$, respectively. We also measured the spike amplitude (A) and duration ($t_{½}$), the AHP amplitude of the first and second action potentials of the discharges, and the resting membrane potentials (V_{rmp}) and input resistances (R_{in}), as previously described (see Cauli et al., 1997 for details).

Means of elicited EPSCs were obtained by averaging the traces after the first presynaptic action potential was aligned using automatic peak detection. Traces not showing postsynaptic responses >150% of the noise level were considered failures. The mean rise time (20–80%) of EPSCs calculated by averaging the synaptic currents without failures was 0.33 ± 0.06 msec ($n = 29$) and 0.28 ± 0.06 msec ($n = 15$) in 3- and 5-week-old rats, respectively. No significant correlation was found between the mean rise time and the averaged amplitude or decay time constant of the EPSCs, indicating a low filtering of the elicited synaptic current in the connections studied ($p > 0.05$; Student's t test).

To examine the paired-pulse response characteristics of the EPSCs, pairs of single action potentials were elicited in presynaptic cells by applying two short depolarizing current pulses separated usually by 50 msec, at different frequencies of stimulation (1 and 0.2 Hz). The paired-pulse response was studied by measuring the amplitudes of the first EPSC (EPSC1) and second EPSC (EPSC2) from the baseline preceding each EPSC and by calculating the ratio amplitude EPSC2/amplitude EPSC1. We tested the recovery from depression and the recovery from facilitation of the elicited responses by varying the interspike interval (from 15 to 200 msec) at stimulation rates of 1 and 0.2 Hz. The coefficient of variation was calculated after baseline noise subtraction by dividing the SD by the mean.

Statistics. The statistical significance of the difference between means of two unpaired samples was computed with the nonparametrical Mann–Whitney U test. The Wilcoxon t test was used to compare the means of two related samples, and correlations between these samples were tested with the nonparametrical Spearman test. For data presenting too many ties, the statistical significance of the means was analyzed with a Student's t test. Statistical data are given as mean ± SD.

Morphology. The slices containing biocytin-filled cells were fixed overnight in 4% paraformaldehyde and 0.2% glutaraldehyde in 0.1 M phosphate buffer (PB) at 4°C. Then, they were rinsed extensively with PB including an intermediate blocking step for endogenous peroxidase activity with 1% H_2O_2 (in PB). The next step was an incubation in a cryoprotectant (30% saccharose in PB) for 1 hr. Then, the slices were freeze-thawed three times over liquid nitrogen. After three rinses in PB, the slices were incubated with ABC (1:200; Vector Laboratories, Burlingame, CA) overnight at 4°C. Thereafter, 1 mg/ml 3,3′ diaminobenzidine (Sigma, St. Louis, MO) was preincubated for 10 min, and then the peroxidase was revealed by starting the reaction with 0.01% H_2O_2. The reaction was stopped by rinsing with PB, and the slices were resectioned on a vibratome to sections of 50 μm thickness. These were intensified with 1% OsO_4 (in PB) for 1 hr, dehydrated in an ascending series of ethanol (including contrasting with 1% uranyl acetate in 70% ethanol for 45 min). After immersion in propylene oxide, the sections were flat-embedded in Durcupan ACM (Fluka, Buchs, Switzerland). Sections were examined with a Zeiss Axioplan equipped with a drawing tube and a 100× oil immersion objective.

RESULTS

We studied the presynaptic and postsynaptic properties of pyramidal cell to FS interneuron connections by using paired recordings at two different postnatal developmental stages. The excitatory synaptic transmission at this identified central synapse was examined in 40 pairs of cells from 3-week-old rats and in 25 pairs of 5-week-old rats. Presynaptic pyramidal cells were impaled with sharp intracellular microelectrodes, and unitary EPSCs were recorded in FS cells with patch pipettes in layer V of the motor cortex (see Materials and Methods).

Identification of the pyramidal cell to FS putative basket interneuron connections

Interneurons of the neocortex are characterized by a large morphological and functional diversity. To restrict our analysis to a single discrete subpopulation, we therefore included in the present study only the FS cells located in layer V that had an apparent multipolar shape as seen with infrared videomicroscopy and nonaccommodating fast-spiking discharges as a physiological hallmark. Figure 1*B* illustrates the firing behavior of the postsynaptic nonpyramidal cells retained in the present study. This neuron emitted a single action potential at the beginning of a near-threshold current pulse, followed by a silent period and a discharge of nonaccommodating fast action potentials. At higher stimulation intensities, all FS cells exhibited continuous high-frequency discharges (Fig. 1*B*, *top trace*). The instantaneous firing frequency during such repetitive discharges was usually >100 Hz and showed limited accommodation at all tested stimulation intensities (Table 1; Fig. 1*B*, *top trace*; see Materials and Methods). In addition, all postsynaptic cells taken into consideration had short spike durations ($t_{½}$), large afterhyperpolarizations (AHPs), small input resistances (R_{in}), and hyperpolarized resting membrane potentials (V_{rmp}; Table 1). These electrophysiological properties are characteristic of FS nonpyramidal cells in the neocortex (Kawaguchi, 1995; Cauli et al., 1997).

All recorded FS neurons that were successfully stained by biocytin injection ($n = 16$; see Materials and Methods) were interneurons located in layer V that possessed round to ovoid somata (largest diameter ranging from 15.3 to 23.1 μm). From the cell body 4–8 smooth, partially beaded primary dendrites originated with variable orientations (Fig. 2*A*,*B*), although with a bias of ramifying more intensely within the infragranular layers. The axon was emitted toward the pia and branched soon and repeatedly, providing a dense field of boutons, typical of extended local plexus cells that are regarded to be putative basket cells (Kawaguchi and Kubota, 1998). In two of 16 cases we were able to identify multiple axosomatic contacts, forming a pericellular basket around unstained cells (Fig. 2*C*). In most other cases only single axosomatic contacts were found to be established by the interneuron axons (putative basket cells; Buhl et al., 1997; Tamas et al., 1997).

Pyramidal cells were initially identified by their characteristic action potential firing induced by depolarizing current pulses (McCormick et al., 1985; Connors and Gutnick, 1990). As seen in Figure 1*A*, pyramidal cells were mainly characterized by a strong firing accommodation (>80%), small AHPs (less than −7 mV), and a long spike duration (>1.5 msec) (see Cauli et al., 1997 for details). In some experiments, biocytin was injected in putative pyramidal cells synaptically connected to FS interneurons. The eight successfully stained presynaptic neurons were all large layer V pyramidal cells with densely spiny dendrites (Fig. 2*A*). Their axons extended from the basal pole of their soma and ran toward the white matter giving off numerous recurrent collaterals forming one or two putative contacts onto primary or secondary dendrites of the FS neuron (Fig. 2*A*,*B*,*D*).

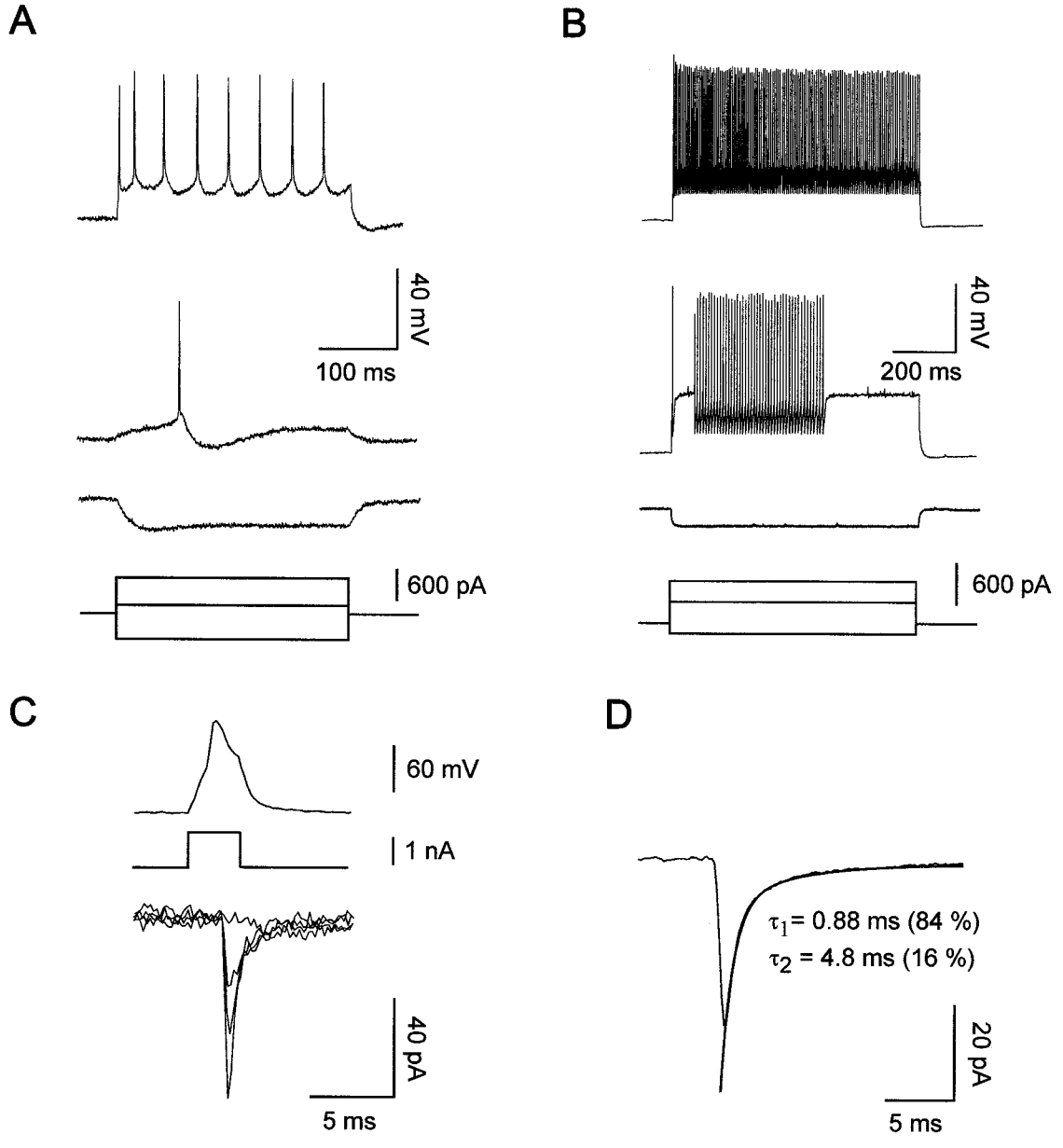

Figure 1. Electrophysiological characterization of connected pyramidal cells and FS interneurons from 18-d-old rats. *A*, Current-clamp recordings of a pyramidal cell during injection of current pulses with a sharp intracellular electrode. In response to near-threshold current pulses, the pyramidal cell emitted a single action potential with a slow AHP (*middle voltage trace*). Note the slow action potentials and the accommodation of the firing during larger depolarizing current pulses (*top voltage trace*) and the time-dependent rectification in response to hyperpolarizing current pulses (*bottom voltage trace*). Recordings are from the pyramidal cell shown in Figure 2*A*. *B*, Current-clamp recordings of a FS interneuron during injection of current pulses with a patch pipette. In response to near-threshold current pulses (*middle voltage trace*), this FS cell emitted a single fast action potential with a large fast AHP followed by a silent period and a late discharge of action potentials. Application of a larger depolarizing current (*top voltage trace*) induced a continuous discharge at high frequency. Note the low input resistance of the FS neuron as seen in response to hyperpolarizing current pulses (*bottom voltage trace*). Recordings are from the FS cell shown in Figure 2*B–D*. *C*, Unitary EPSCs at a pyramidal–FS connection. The *top trace* illustrates an action potential elicited in the pyramidal neuron by a brief depolarizing current pulse (*middle voltage trace*). The *bottom traces* are four superimposed current responses recorded in the FS interneuron at a holding potential of −72 mV during the stimulation of the pyramidal neuron. Note an apparent transmission failure and the large variation of the EPSC amplitudes. Recordings are from the connection illustrated in Figure 2*B–D*. *D*, Kinetics of unitary EPSCs at the same pyramidal–FS connection as in *C*. A biexponential fit of the decay of the EPSC was superimposed to the average of 203 postsynaptic responses, excluding failures. The *numbers* in *parentheses* represent the relative amplitude of the first (τ_1) and the second (τ_2) exponential.

Functional properties of neocortical pyramidal to fast-spiking connections

For all connected pairs, action potentials elicited in the presynaptic pyramidal cell induced unitary postsynaptic responses in the FS interneuron that had short latencies, low failure rates, and large coefficients of variation (Tables 1, 2; Fig. 1*C*). At a holding potential of −72 mV the average EPSC was rapidly rising and decaying (Fig. 1*D*) and was almost completely abolished by 10 μM NBQX or DNQX, two competitive antagonists of AMPA/kainate receptors (Table 1). The decay of the average EPSC was adequately fitted in 37 of 54 pairs by a double exponential function (Table 1, Fig. 1*D*). The amplitude of the second expo-

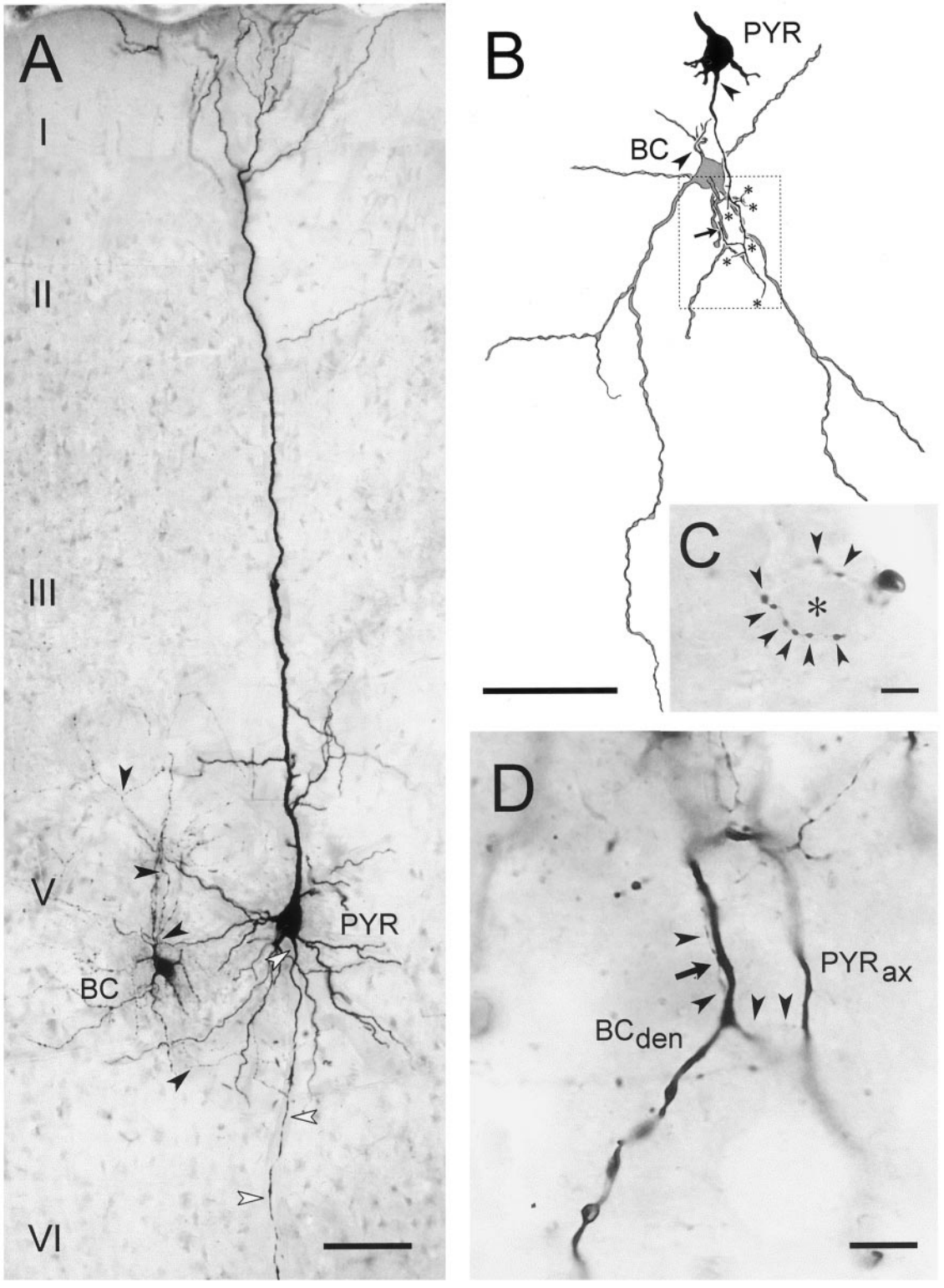

Figure 2. Morphological characterization of pyramidal–FS connections from 18-d-old rats. *A*, Photomontage of a typical pyramidal cell (*PYR*) to a putative basket cell (*BC*) connection as recorded and stained with biocytin in the present study. Both cells have large somata located in layer V of motor cortex and possess a characteristic morphology for the respective cell class. *White arrowheads* mark the axon of the pyramidal cell, *black arrowheads* those of the interneuron. *Roman numerals* denominate cortical laminae. *B*, Camera lucida drawing showing the contact formed by another pair, also from layer V. The soma of the pyramidal cell and the skeleton of the axon until it contacts a secondary dendrite of the large multipolar putative basket cell (*arrow*) is traced. Axonal branch points that have not been reconstructed further are marked with an *asterisk*. *Arrowheads* indicate the axon initial segments of both cells. *Stippled frame* marks area shown as micrograph in *D*. *C*, Basket-like terminal formation of the axon of the interneuron shown in *B*. *Arrowheads* point to individual boutons presumably contacting the encircled soma (*asterisk*). *D*, High-power micrograph showing the pyramidal cell axon (PYR_{ax}), specifically the course of the recurrent collateral (*arrowheads*) that forms a delicate contact (*arrow*) with the putative basket cell dendrite (BC_{den}). Scale bars: *A*, *B*, 100 μm; *C*, *D*, 10 μm.

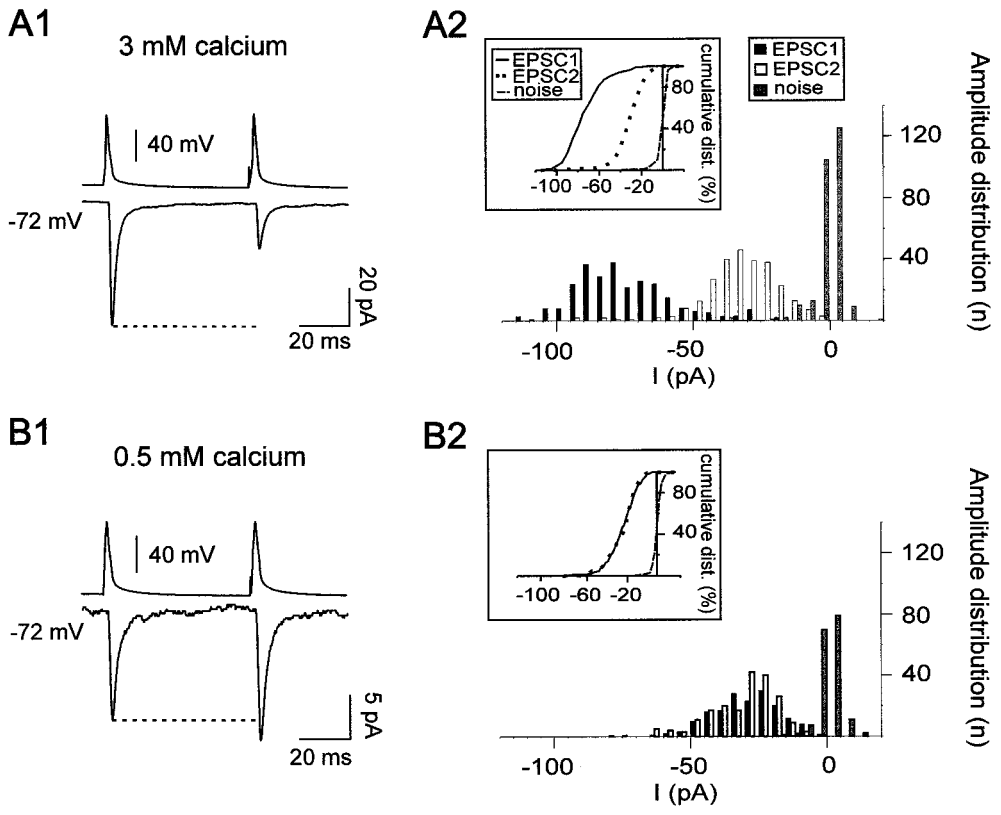

Figure 3. Multiple quanta of transmitter released at a single pyramidal–FS connection from a 16-d-old rat. *A1*, *B1*, The *bottom traces* show the mean amplitude, including failures, of the postsynaptic currents (EPSC1 and EPSC2) recorded in a FS cell in response to pairs of action potentials (*top traces*) elicited in a presynaptic pyramidal cell with an interspike interval of 50 msec at a stimulation rate of 1 Hz in 3 mM (*A1*) and 0.5 mM (*B1*) of $[Ca^{2+}]_e$. A marked PPD (ratio of 0.37) was observed in 3 mM $[Ca^{2+}]_e$ (*A1*), whereas a PPF (ratio of 1.2) was obtained when reducing $[Ca^{2+}]_e$ to 0.5 mM (*B1*). The response probabilities of EPSC1 and EPSC2 were, respectively, 0.99 and 0.88 in 3 mM $[Ca^{2+}]_e$ and 0.52 and 0.6 in 0.5 mM $[Ca^{2+}]_e$. Traces are averages of 270 and 330 responses for *A1* and *B1*, respectively. *A2*, *B2*, Amplitude distributions of EPSC1 and EPSC2, excluding failures, obtained in 3 mM $[Ca^{2+}]_e$ (*A2*) and 0.5 mM $[Ca^{2+}]_e$ (*B2*). The histograms and cumulative plots (*A2*, *inset*) show that the distribution of EPSC1 and EPSC2 were significantly different in 3 mM $[Ca^{2+}]_e$, suggesting that multiple quanta were released at this connection. This was confirmed by the reduction in amplitude of both responses in 0.5 mM $[Ca^{2+}]_e$ (*B2*, *inset*). In low $[Ca^{2+}]_e$, the amplitude distribution of EPSC1 and EPSC2 were identical suggesting that, under these conditions of low release probability, a single quantum was released when there was a response (*B2*). An apparent quantal size of −20 pA could be estimated from the current corresponding to 50% of the cumulative distribution (*B2*, *inset*).

nential represented only a minor portion of the total current, indicating a predominance of the fastest component (Table 1). The EPSCs of 17 connections were best fitted with a single exponential function (Table 1). We did not observe any significant difference between pyramidal–FS connections from 3- and 5-week-old rats as far as the peak amplitudes and the first and second decay time constants of AMPA receptor-mediated unitary EPSCs were concerned (Table 1; $p > 0.05$; Mann–Whitney *U* test). In agreement with previous observations (Angulo et al., 1997), the *I–V* plot of the AMPA receptor-mediated unitary EPSCs showed an inward rectification between −20 and +40 mV (M. C. Angulo, J. Rossier, and E. Audinat, unpublished observations), characteristic of calcium-permeable AMPA receptors (for review, see Jonas and Burnashev, 1995).

To determine whether pyramidal–FS connections consisted of single or multiple release sites, we manipulated the release probabilities by using paired-pulse stimulations of presynaptic cells and by changing the concentration of $[Ca^{2+}]_e$.

Figure 3 illustrates the average responses, including failures, recorded in a FS interneuron by spike pairs elicited in a pyramidal cell with an interspike interval of 50 msec at a stimulation rate of 1 Hz. The comparison of the average amplitude, including failures, of EPSC1 to that of EPSC2 indicated that this connection showed a paired-pulse depression (Fig. 3*A1*). The paired-pulse ratio (amplitude EPSC2/amplitude EPSC1) was 0.37. Failure rates at EPSC1 and EPSC2 were 0.01 and 0.12, respectively, indicating different release probabilities at the first and second spikes. The amplitude distribution of EPSC1 and EPSC2 significantly differed with EPSC1 amplitudes centered around larger values (Fig. 3*A2*, *inset*; $p < 0.0001$; Wilcoxon *t* test). Consequently, the mean amplitude of EPSC1 excluding failures was larger than that of EPSC2 (data not shown). These observations suggest that more vesicles were released at the first than at the second presynaptic action potential (Stevens and Wang, 1995). If no more than one vesicle is released at each site (for review, see Redman, 1990; Korn and Faber, 1991), then this indicates that this synapse consisted of several release sites.

In 44 pyramidal–FS connections from 3-week-old ($n = 33$) and 5-week-old ($n = 11$) animals, in which paired-pulse protocols were applied, we observed a significant difference between the average amplitude, excluding failures, of EPSC1 and EPSC2 (Table 2; $p < 0.001$; Wilcoxon *t* test). These results suggest that, at both investigated developmental stages, pyramidal–FS connections mainly consist of multiple functional release sites. For six connections from 3-week-old ($n = 1$) and 5-week-old ($n = 5$) rats, the amplitudes, excluding failures, and probabilities of response

Table 2. Paired-pulse response characteristics of pyramidal–FS connections at two different developmental stages

	Connections from 3-week-old rats mean ± SD (*n*)	Connections from 5-week-old rats mean ± SD (*n*)
Stimulation rate of 1 Hz[a]		
Amp. EPSC1	−41 ± 30 pA (38)	−43 ± 54 pA (19)
Amp. EPSC2	−22 ± 13 pA (38)	−33 ± 43 pA (19)
CV[b] EPSC1	35 ± 18% (29)	46 ± 18% (15)
CV[b] EPSC2	42 ± 19% (29)	49 ± 22% (15)
Amp. EPSC1 excluding failures	−47 ± 27 pA (38)	−53 ± 55 pA (19)
Amp. EPSC2 excluding failures	−29 ± 14 pA (38)	−43 ± 44 pA (19)
Prob. resp. EPSC1[c]	0.75 ± 0.21 (8)	0.79 ± 0.25 (11)
Prob. resp. EPSC2[c]	0.63 ± 0.25 (8)	0.80 ± 0.21 (11)
Paired-pulse ratio	0.6 ± 0.2 (38)	0.87 ± 0.4 (19)
Stimulation rate of 0.2 Hz[a]		
Amp. EPSC1	−24 ± 14 pA (8)	−43 ± 52 pA (13)
Amp. EPSC2	−14 ± 10 pA (8)	−50 ± 62 pA (13)
CV[b] EPSC1	29 ± 19% (6)	32 ± 26% (6)
CV[b] EPSC2	51 ± 24% (6)	37 ± 17% (6)
Amp. EPSC1 excluding failures	−30 ± 15 pA (8)	−49 ± 56 pA (11)
Amp. EPSC2 excluding failures	−20 ± 11 pA (8)	−55 ± 68 pA (11)
Prob. resp. EPSC1[c]	0.84 ± 0.16 (8)	0.8 ± 0.25 (11)
Prob. resp. EPSC2[c]	0.77 ± 0.16 (8)	0.84 ± 0.2 (11)
Paired-pulse ratio	0.59 ± 0.12 (8)	1.21 ± 0.43 (15)
Low external calcium concentration (stimulation rate of 1 Hz)[a]		
Amp. EPSC1	−5 ± 5 pA (8)	−8.6 and −0.8 pA (2)
Amp. EPSC2	−7 ± 5 pA (8)	−8.5 and −1.3 pA (2)
Amp. EPSC1 excluding failures	−22 ± 8 pA (8)	−33.6 and −11.3 pA (2)
Amp. EPSC2 excluding failures	−24 ± 9 pA (8)	−32.7 and −11.9 pA (2)
Prob. response EPSC1	0.3 ± 0.14 (6)	0.34 and 0.05 (2)
Prob. response EPSC2	0.4 ± 0.14 (6)	0.35 and 0.06 (2)
Paired-pulse ratio	1.5 ± 0.4 (8)	1 and 1.6 (2)

[a]Interspike interval of 50 msec.

[b]CV, coefficient of variation.

[c]The reported probabilities of response correspond to those obtained at connections tested at both stimulation rates (1 and 0.2 Hz). The differences of the probability of response between 1 and 0.2 Hz were tested only with connections at which both stimulation rates were obtained.

of EPSC1 and EPSC2 were identical, and therefore it was not possible to determine whether they consisted of single or multiple release sites.

The effect of decreasing the $[Ca^{2+}]_e$ to 0.5 mM was studied on paired-pulse responses elicited at a stimulation rate of 1 Hz. As shown in the example of Figure 3*B*, after changing to a low calcium-containing bathing solution, the proportion of failures increased and became higher for EPSC1 than for EPSC2, leading to a switch from depression to facilitation (Table 2). In addition, the amplitude of the EPSCs decreased as shown by the shift of EPSC1 and EPSC2 amplitude distributions toward smaller values (Fig. 3*B2*, *inset*; $p < 0.0001$; Mann–Whitney *U* test). This decrease in response probabilities associated with a decrease of the average amplitude without failures for both EPSC1 and EPSC2 when lowering $[Ca^{2+}]_e$ was also observed in nine other connections (Table 2; $p < 0.025$; Wilcoxon *t* test). In four cases, these changes could be reversed after restoration of normal $[Ca^{2+}]_e$ (data not shown).

For four of the 10 connections from 3-week-old ($n = 3$) and 5-week-old ($n = 1$) animals for which we lowered the $[Ca^{2+}]_e$ to 0.5 mM, as in the example of Figure 3, we observed no statistical differences between the cumulative amplitude distributions of EPSC1 and EPSC2 in low $[Ca^{2+}]_e$ (Fig. 3*B2*, *inset*), although the probabilities of the two responses differed ($p > 0.05$; Mann–Whitney *U* test). This suggested that in these conditions only one quantum of transmitter was released on the average when there was a response. The mean amplitude of the EPSCs without failures recorded at these four connections in low $[Ca^{2+}]_e$ corresponded to the postsynaptic response to one quantum of transmitter, i.e., the apparent quantal size, which varied from 11 to 29 pA with a mean of 19 ± 8 pA ($n = 4$). These values are within those reported by Bolshakov and Siegelbaum (1995) and Geiger et al. (1997) at excitatory synapses in the hippocampus. The ratio of the mean amplitude of EPSC1 without failures in normal $[Ca^{2+}]_e$ over the apparent quantal size obtained in low $[Ca^{2+}]_e$, gives a quantal content of 1.8, 1.9, 2.5, and 3.1 (mean, 2.3 ± 0.6).

These results indicate that the average number of release sites active at each response decreased when lowering $[Ca^{2+}]_e$ and confirm that pyramidal–FS connections in slices of both 3- and 5-week-old rats consist of multiple functional release sites.

Postnatal development of the activity-dependent properties of synaptic transmission at pyramidal–FS connections

As mentioned above, most of the pyramidal–FS connections examined at a stimulation rate of 1 Hz displayed PPD when pairs of presynaptic action potentials were elicited with an interspike interval of 50 msec (in 2 or 3 mM $[Ca^{2+}]_e$). The pooled data from

connections from 3-week-old ($n = 38$) and 5-week-old ($n = 21$) rats indicated, however, that the depression was more marked at connections obtained in slices from younger rats (Table 2; $p < 0.01$; Mann–Whitney U test). Larger PPD also occurred in connections of the young compared with the older animals when interspike intervals of 15, 100, and 200 msec were used (Fig. 4*E*). For both developmental stages, PPD decreased between intervals of 15 and 200 msec (Fig. 4*E*) but this decrease of PPD was only significant at connections from 3-week-old animals ($p < 0.025$; Mann–Whitney U test).

We then investigated the effects of spike pairs elicited at two different stimulation rates (1 and 0.2 Hz). Figure 4*A* illustrates the responses to paired-pulse stimulations elicited at 1 Hz (Fig. 4*A1*) and 0.2 Hz (Fig. 4*A2*) at a pyramidal–FS connection from a 19-d-old animal, using an interspike interval of 50 msec. In both cases a depression of the second response was observed with a paired-pulse ratio of 0.64 and 0.73 at 1 and 0.2 Hz, respectively. For eight tested connections from 3 week-old rats, there were no significant differences in the paired-pulse ratio obtained at the two frequencies (Fig. 4*C*; $p > 0.05$; Wilcoxon t test). The response probability of EPSC1 and of EPSC2 was, however, larger at a low rate of stimulation (Table 2; $p < 0.01$; Wilcoxon t test).

At pyramidal–FS connections from 5-week-old rats, the response probability of EPSC1 was not affected by the rate of stimulation, but for EPSC2 the response probability increased significantly when the stimulation rate decreased from 1 to 0.2 Hz (Table 2; $p < 0.01$; Wilcoxon t test). This modification induced an increase in the paired-pulse ratio in all 15 tested connections from 5-week-old rats (Fig. 4*C*; $p < 0.001$; Wilcoxon t test) leading in eight cases to a switch from a PPD at a stimulation rate of 1 Hz, to a PPF when the spike pairs were delivered at a stimulation rate of 0.2 Hz (Fig. 4*B1*,*B2*). The plot of all individual data shown in Figure 4*D* illustrates the large variability of the paired-pulse responses and the predominance of facilitation at lower stimulation rates at connections from 5-week-old rats. For five connections that facilitated at a stimulation rate of 0.2 Hz, pairs of action potentials were applied at different interspike intervals (Fig. 4*F*). PPF was large at intervals of 15 msec (average paired-pulse ratio of 1.74 ± 0.8) but was not observed at intervals of 200 msec (Fig. 4*F*; $p < 0.05$; Mann–Whitney U test).

Differential functional maturation of pyramidal–FS connections

The modifications of the activity-dependent short-term effects at pyramidal–FS connections observed between the third and fifth postnatal week occurred without significant changes of the kinetics of the AMPA receptor-mediated unitary EPSCs (see above and Table 1). At a stimulation rate of 0.2 Hz, there were no significant differences either in the response probabilities or in the average amplitude of EPSC1 with or without failures between the two developmental stages (Table 2; $p > 0.05$; Mann–Whitney U test).

The restricted distribution of the paired-pulse ratios in our sample of connections in young animals (Fig. 4*D*) suggested that all pyramidal cell inputs to FS cells have similar paired-pulse characteristics. However, the large distribution observed in the sample of connections in 5-week-old animals may imply that different pyramidal cell inputs onto the same FS cell evolved differently. This has been directly tested by comparing the synaptic properties of two different presynaptic pyramidal cells impinging onto the same postsynaptic FS interneuron.

Figure 5*A* illustrates the paired-pulse responses of a single postsynaptic FS cell from a 33-d-old rat elicited by two different presynaptic pyramidal neurons at a stimulation rate of 0.2 Hz. The first connection onto this postsynaptic cell showed a depression (ratio of 0.64), whereas the second one showed a facilitation (ratio of 1.4). In two of three other sequential paired recordings in slices of 5-week-old rats, the input from one pyramidal cell displayed a PPD, whereas the input from another pyramidal cell was characterized by a PPF (Fig. 5*B*). In contrast, when sequential paired recordings were performed in four postsynaptic young FS cells (eight connections), we always observed a PPD (Fig. 5*B*).

These results show that, at the end of the first postnatal month, inputs from different pyramidal cells onto the same FS interneuron have different paired-pulse response characteristics, suggesting that the regulation of glutamate release mechanisms differs among pyramidal cells.

DISCUSSION

Paired recordings in neocortical slices indicate that pyramidal–FS connections consist of multiple release sites at which AMPA receptors mediate most of the postsynaptic current near resting membrane potentials. These synapses always display PPD at early stages of postnatal development. At later stages of development, short-term adjustments in the synaptic gain during repetitive activity can lead to either depression or facilitation according to the presynaptic firing rate. These results indicate that critical synaptic parameters for short-term plasticity at this excitatory neocortical connection mature relatively late during postnatal development.

Basic properties of pyramidal–FS connections

We found that transmitter release fluctuated randomly at pyramidal–FS connections and that the amplitude distribution of unitary synaptic responses was modified by manipulations affecting the probability of release such as paired-pulse protocols or changes in $[Ca^{2+}]_e$. This therefore suggests that single presynaptic action potentials trigger the release of several quanta of glutamate at pyramidal–FS connections. Our morphological estimation of the number of synaptic junctions (one or two putative contacts; $n = 4$) is comparable with the study reported by Buhl et al. (1997) at pyramidal–basket cell connections in the adult visual cortex of the cat. These numbers of morphological contacts are of the same order of magnitude as the number of quanta released that can be estimated from our physiological data by comparing the quantal size obtained in low $[Ca^{2+}]_e$ to the amplitude of the control EPSC (2.3 quanta on average; $n = 4$). Both methods probably lead to an underestimation of the number of release sites because, on the one hand, some contacts can be obscured during morphological analysis (e.g., by axons undercrossing dendrites) and, on the other hand, the probability of release at each site is probably <1 at physiological $[Ca^{2+}]_e$. All together, these observations show that pyramidal–FS connections consist of multiple release sites.

Postnatal development of activity-dependent properties of synaptic transmission at pyramidal–FS connections

Conflicting results concerning the modifications of synaptic strength that occur in response to paired-pulse protocols or short trains of presynaptic action potential at pyramidal–FS or pyramidal–basket cell connections have been published previously. Thomson et al. (1993, 1995) first showed a profound frequency-dependent facilitation at pyramidal cell inputs onto interneurons, including FS cells, in the adult rat neocortex. More recently, Buhl

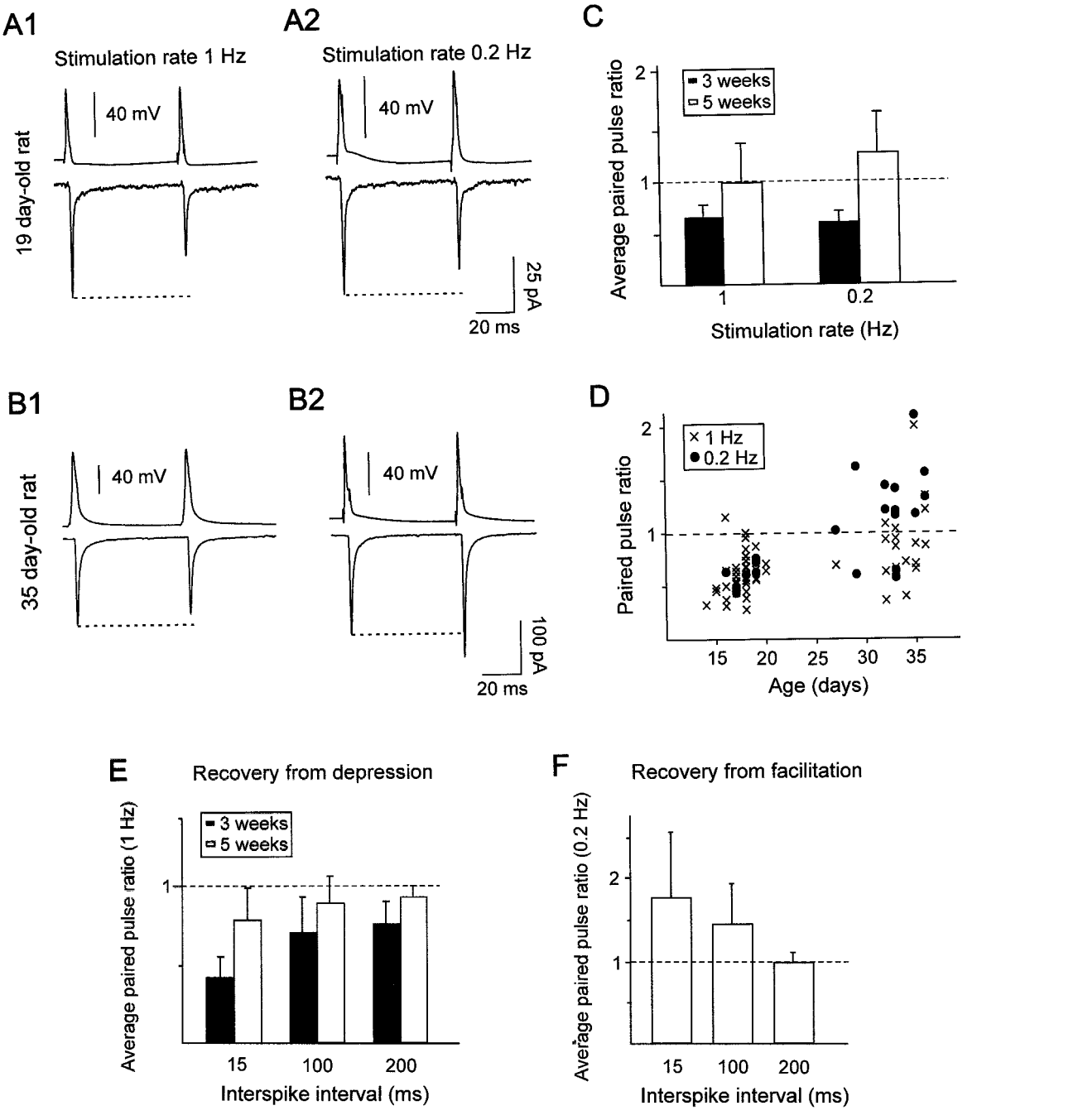

Figure 4. Paired-pulse response characteristics at pyramidal–FS connections at two different developmental stages. *A*, *B*, Paired-pulse responses elicited with a presynaptic interspike interval of 50 msec (*top traces*) at stimulation rates of 1 (*A1*, *B1*) and 0.2 Hz (*A2*, *B2*) in FS interneurons from 19- and 35-d-old rats. The *bottom traces* correspond to the mean amplitudes, including failures, of the postsynaptic currents. For the connection in *A*, the response probabilities of EPSC1 and EPSC2 were, respectively, 0.96 and 0.93 at a stimulation rate of 1 Hz (*A1*) and 1 and 0.98 at a stimulation rate of 0.2 Hz (*A2*). For the connection in *B*, the response probabilities of EPSC1 and EPSC2 were, respectively, 0.99 and 1 at a stimulation rate of 1 Hz (*B1*) and 1 at a stimulation rate of 0.2 Hz (*B2*). Note that in *A* the connection showed a PPD at stimulation rates of 1 Hz (ratio of 0.64) and 0.2 Hz (ratio of 0.73), whereas in *B* the connection showed a PPD at a stimulation rate of 1 Hz (ratio of 0.89) and a PPF at 0.2 Hz (ratio of 1.2). Traces are averages from 69 to 131 responses. *C*, Average of the paired-pulse ratios at connections from 3-week-old rats (*black bars*) and 5-week-old rats (*white bars*). Only pairs tested at both stimulation rates were included. There was a statistical difference between the ratios obtained at 1 and 0.2 Hz for pairs from 5-week-old rats ($p < 0.001$; $n = 11$) but not for pairs from younger animals ($n = 8$). Note that the PPD was more marked at connections from younger animals. *D*, Plot of the paired-pulse ratio of all individual connections as a function of the age of the preparation at stimulation rates of 1 Hz (*crosses*; $n = 57$) and 0.2 Hz (*circles*; $n = 23$). Note the large variability of responses at pairs from 5-week-old animals. *E*, Recovery from depression. Average paired-pulse ratios at connections from 3-week-old ($n = 5$) and 5-week-old ($n = 6$) rats obtained at presynaptic interspike intervals of 15, 100, and 200 msec at a stimulation rate of 1 Hz. *F*, Recovery from facilitation. Average paired-pulse ratios at connections from 5-week-old rats ($n = 5$) obtained at presynaptic interspike intervals of 15, 100, and 200 msec at a stimulation rate of 0.2 Hz.

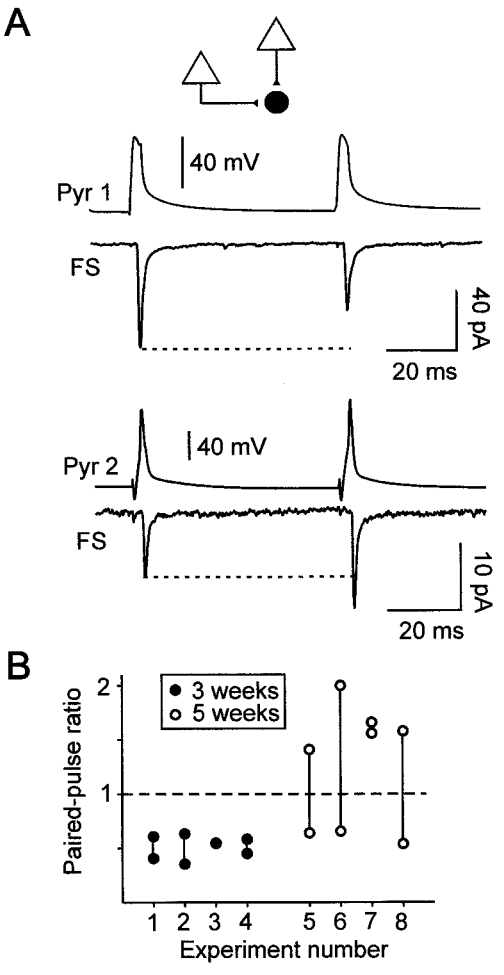

Figure 5. Paired-pulse responses elicited by two different presynaptic pyramidal cells onto single postsynaptic FS interneurons. *A*, Paired-pulse responses of a FS interneuron elicited by two presynaptic pyramidal cells recorded sequentially in a slice from a 33-d-old rat. A PPD (ratio of 0.64; traces are averages of 50 responses) was observed at the first connection (*Pyr 1-FS*) at which the response probabilities of EPSC1 and EPSC2 were 0.94 and 0.86, respectively. A PPF (ratio of 1.4; traces are averages of 76 responses) was observed at the second connection (*Pyr 2-FS*) with response probabilities of 0.7 and 0.87 for EPSC1 and EPSC2, respectively. *B*, Comparison of the paired-pulse ratios of two different presynaptic inputs onto single FS interneurons. *Vertical lines* link the two data points corresponding to the paired-pulse ratios of the two connections studied for each of the eight FS cells recorded in 3-week-old ($n = 4$) and 5-week-old ($n = 4$) animals. Note that PPD was obtained at all young connections, whereas different inputs onto three of four single FS cells from 5-week-old rats could display either PPD or PPF. It is noteworthy that, at older connections, the presence of PPD or PPF was independent of the order in which the sequential connections were obtained.

et al. (1997) reported PPD at pyramidal-to-basket cell synapses in the adult cat visual cortex, and Reyes et al. (1998) also described depression at synapses between pyramidal cells and FS putative basket cells in the young rat neocortex. These data can be simply reconciled, in light of our present results, by taking into account the differences in the stimulation rates and the ages of the animals used by the different authors. Indeed, our results clearly show that PPD is predominant in young animals within a large range of stimulation rates. At the fifth postnatal week, most pyramidal–FS connections of our sample can display PPF at low stimulation rates (0.2 Hz) and PPD at higher rates (1 Hz). It is not excluded, however, that conflicting results between authors rely also on different experimental protocols and conditions. In particular, trains of presynaptic action potentials have been used by some authors (Thomson, 1997; Reyes et al., 1998), whereas others have quantified the effects of paired-pulse protocols (Buhl et al., 1997).

Postnatal changes of paired-pulse response characteristics of neocortical excitatory synapses have never been reported previously. At excitatory synapses between CA3 and CA1 hippocampal pyramidal cells, Bolshakov and Siegelbaum (1995) showed a decrease in the probability of release without postsynaptic modifications between the first and third postnatal weeks. At inhibitory synapses between interneurons and Purkinje cells in the cerebellar cortex, the decrease of the average unitary synaptic current amplitude observed between the second and the fifth postnatal weeks seemed to involve both presynaptic and postsynaptic modifications (Pouzat and Hestrin, 1997). In both cases, a switch from PPD to PPF accompanied these developmental changes of synaptic transmission. We did not observe significant modifications of the unitary EPSC kinetics and amplitudes between the third and fifth postnatal weeks that could suggest a change in the properties of the postsynaptic AMPA receptors. The switch from PPD to PPF at low stimulation rates (0.2 Hz) during the postnatal development at pyramidal–FS connections strongly suggests the occurrence of presynaptic modifications.

The observation that, in 3-week-old rats, all pyramidal cell inputs onto single FS interneurons always displayed PPD is in agreement with recent data showing that the different natures of the target neurons underlie the early development of presynaptic properties determining the facilitating or depressing characteristics of hippocampal or neocortical synapses (Markram et al., 1998; Reyes et al., 1998; Scanziani et al., 1998). Our results indicate that the homogeneity of presynaptic properties in young animals, as determined by these target-specific mechanisms, evolves toward a more complex situation during later stages of development. Indeed, inputs from different pyramidal cells onto the same FS interneuron had different paired-pulse response characteristics that differed not only quantitatively (Markram et al., 1998) but also qualitatively because some inputs could display PPD and others PPF. This suggests that the postnatal development and more recent activity endow each pyramidal–FS connection with unique functional properties in the neocortical network at the end of the first postnatal month. We cannot exclude, however, that the heterogeneity of the paired-pulse responses observed at 5-week-old animals indicates that pyramidal–FS connections are still on the course of development.

Physiological implications

At most pyramidal–FS connections from 5 week-old rats, the paired-pulse ratio resulting from the coexisting facilitation and depression mechanisms will vary within a wider range than at younger connections, endowing older connections with large integrative capabilities. This balance between facilitation and depression is determined by the activity of the presynaptic pyramidal cells which *in vivo* can adopt a wide range of frequencies, often irregular (for references, see Softky and Koch, 1993). Pyramidal cell inputs to FS cells *in vivo* are therefore likely to consist of sequences of single spikes and small bursts of spikes delivered at a large range of frequencies. Our results predict that the number of presynaptic pyramidal cell inputs needed to activate a FS cell will vary with the overall activity that those inputs had experienced during the preceding seconds. Because of the high reciprocal connectivity between pyramidal cells and FS cells (Reyes et al., 1998), it is likely that a single FS cell is involved in an

extremely large number of recurrent inhibitory loops. The observation that synaptic transmission at pyramidal–FS connections is facilitated or depressed depending on the presynaptic firing rate suggests that the relative weight of the recurrent inhibition mediated by a given FS cell in different loops is dynamically adjusted.

REFERENCES

Angulo MC, Lambolez B, Audinat E, Hestrin S, Rossier J (1997) Subunit composition, kinetic, and permeation properties of AMPA receptors in single neocortical nonpyramidal cells. J Neurosci 17:6685–6696.

Bolshakov VY, Siegelbaum SA (1995) Regulation of hippocampal transmitter release during development and long-term potentiation. Science 269:1730–1734.

Buhl EH, Tamas G, Szilagyi T, Stricker C, Paulsen O, Somogyi P (1997) Effect, number and location of synapses made by single pyramidal cells onto aspiny interneurones of cat visual cortex. J Physiol (Lond) 500:689–713.

Buzsaki G (1997) Functions for interneuronal nets in the hippocampus. Can J Physiol Pharmacol 75:508–515.

Cauli B, Audinat E, Lambolez B, Angulo M-C, Ropert N, Tsuzuki K, Hestrin S, Rossier J (1997) Molecular and physiological diversity of cortical nonpyramidal cells. J Neurosci 17:3894–3906.

Cobb SR, Buhl EH, Halasy K, Paulsen O, Somogyi P (1995) Synchronization of neuronal activity in hippocampus by individual GABAergic interneurons. Nature 378:75–78.

Connors BW, Gutnick MJ (1990) Intrinsic firing patterns of diverse neocortical neurons. Trends Neurosci 13:99–104.

Davis GW, Murphey RK (1993) A role for postsynaptic neurons in determining presynaptic release properties in the cricket CNS: evidence for retrograde control of facilitation. J Neurosci 13:3827–3838.

Deuchars J, West DC, Thomson AM (1994) Relationships between morphology and physiology of pyramid-pyramid single axon connections in rat neocortex *in vitro*. J Physiol (Lond) 478:423–435.

Galarreta M, Hestrin S (1998) Frequency-dependent synaptic depression and the balance of excitation and inhibition in the neocortex. Nat Neurosci 1:587–594.

Geiger JR, Lubke J, Roth A, Frotscher M, Jonas P (1997) Submillisecond AMPA receptor-mediated signaling at a principal neuron-interneuron synapse. Neuron 18:1009–1023.

Jonas P, Burnashev N (1995) Molecular mechanisms controlling calcium entry through AMPA-type glutamate receptor channels. Neuron 15:987–990.

Katz PS, Kirk MD, Govind CK (1993) Facilitation and depression at different branches of the same motor axon: evidence for presynaptic differences in release. J Neurosci 13:3075–3089.

Kawaguchi Y (1993) Groupings of nonpyramidal and pyramidal cells with specific physiological and morphological characteristics in rat frontal cortex. J Neurophysiol 69:416–431.

Kawaguchi Y (1995) Physiological subgroups of nonpyramidal cells with specific morphological characteristics in layer II/III of rat frontal cortex. J Neurosci 15:2638–2655.

Kawaguchi Y, Kubota Y (1998) Neurochemical features and synaptic connections of large physiologically-identified GABAergic cells in the rat frontal cortex. Neuroscience 85:677–701.

Koerber HR, Mendell LM (1991) Modulation of synaptic transmission at Ia-afferent fiber connections on motoneurons during high-frequency stimulation: role of postsynaptic target. J Neurophysiol 65:590–597.

Korn H, Faber DS (1991) Quantal analysis and synaptic efficacy in the CNS. Trends Neurosci 14:439–445.

Markram H, Lubke J, Frotscher M, Roth A, Sakmann B (1997) Physiology and anatomy of synaptic connections between thick tufted pyramidal neurones in the developing rat neocortex. J Physiol (Lond) 500:409–440.

Markram H, Wang Y, Tsodyks M (1998) Differential signaling via the same axon of neocortical pyramidal neurons. Proc Natl Acad Sci USA 95:5323–5328.

McCormick DA, Connors BW, Lighthall JW, Prince DA (1985) Comparative electrophysiology of pyramidal and sparsely spiny stellate neurons of the neocortex. J Neurophysiol 54:782–806.

Muller KJ, Nicholls JG (1974) Different properties of synapses between a single sensory neurone and two different motor cells in the leech CNS. J Physiol (Lond) 238:357–369.

Neher E (1992) Correction for liquid junction potentials in patch clamp experiments. Methods Enzymol 207:123–131.

Parra P, Gulyas AI, Miles R (1998) How many subtypes of inhibitory cells in the hippocampus? Neuron 20:983–993.

Pouzat C, Hestrin S (1997) Developmental regulation of Basket/Stellate cell–Purkinje cell synapses in the cerebellum. J Neurosci 17:9104–9112.

Redman S (1990) Quantal analysis of synaptic potentials in neurons of the central nervous system. Physiol Rev 70:165–198.

Reyes A, Lujan R, Rozov A, Burnashev N, Somogyi P, Sakmann B (1998) Target-cell-specific facilitation and depression in neocortical circuits. Nat Neurosci 1:279–285.

Scanziani M, Gähwiler B, Charpak S (1998) Target-cell specific modulation of transmitter release at terminals from a single axon. Proc Natl Acad Sci USA 95:12004–12009.

Softky WR, Koch C (1993) The highly irregular firing of cortical cells is inconsistent with temporal integration of random EPSPs. J Neurosci 13:334–350.

Stevens CF, Wang Y (1995) Facilitation and depression at single central synapses. Neuron 14:795–802.

Stuart GJ, Dodt HU, Sakmann B (1993) Patch-clamp recordings from the soma and dendrites of neurons in brain slices using infrared video microscopy. Pflügers Arch 423:511–518.

Tamas G, Buhl EH, Somogyi P (1997) Fast IPSPs elicited via multiple synaptic release sites by different types of GABAergic neurone in the cat visual cortex. J Physiol (Lond) 500:715–738.

Thomson AM (1997) Activity-dependent properties of synaptic transmission at two classes of connections made by rat neocortical pyramidal axons *in vitro*. J Physiol (Lond) 502:131–147.

Thomson AM, Deuchars J, West DC (1993) Single axon excitatory postsynaptic potentials in neocortical interneurons exhibit pronounced paired pulse facilitation. Neuroscience 54:347–360.

Thomson AM, West DC, Deuchars J (1995) Properties of single axon excitatory postsynaptic potentials elicited in spiny interneurons by action potentials in pyramidal neurons in slices of rat neocortex. Neuroscience 69:727–738.

Tsodyks MV, Markram H (1997) The neural code between neocortical pyramidal neurons depends on neurotransmitter release probability. Proc Natl Acad Sci USA 94:719–723.

Whittington MA, Traub RD, Jefferys JG (1995) Synchronized oscillations in interneuron networks driven by metabotropic glutamate receptor activation. Nature 373:612–615.

Zucker RS (1989) Short-term synaptic plasticity. Annu Rev Neurosci 12:13–31.